Chemistry & Biology, Vol. 12, 323–328, March, 2005, ©2005 Elsevier Ltd All rights reserved. DOI 10.1016/j.chembiol.2005.01.013

Gold Nanoparticles as a Colorimetric Sensor for Protein Conformational Changes

Soonwoo Chah, Matthew R. Hammond, and Richard N. Zare*
Department of Chemistry
Stanford University
Stanford, California 94305

Summary

Spherical gold nanoparticles and flat gold films are prepared in which yeast iso-1-cytochrome c (Cyt c) is covalently bound to the gold surface by a thiol group in the cystein 102 residue. Upon exposure to solutions of different pH, bound Cyt c unfolds at low pH and refolds at high pH. This conformational change causes measurable shifts in the color of the coated nanoparticle solutions detected by UV-VIS absorption spectroscopy and in the refractive index (RI) of the flat gold films detected by surface plasmon resonance (SPR) spectroscopy. Both experiments demonstrate the same trend with pH, suggesting the use of protein-covered gold nanoparticles as a simple colorimetric sensor for conformational change.

Introduction

Conformational changes in proteins, which result from the intrinsic flexibility of their structures, are of major importance in understanding various biomolecular interactions. Such changes have been studied by nuclear magnetic resonance (NMR), X-ray diffraction, Fourier transform infrared (FTIR) spectroscopy, and near-UV circular dichroism (CD) [1–4]. Nevertheless, the need exists to develop simple sensors that can detect conformational changes in proteins when the proteins are exposed to different environments. The fact that proteins immobilized at an interface often behave differently from their counterparts in bulk solution is of additional interest to researchers in this area [5]. We report the use of a colloidal suspension of protein-covered gold nanoparticles for these purposes. Its absorption spectrum serves to measure the extent of conformational change for different solution conditions.

Conformational change in cytochrome c has been studied in the bulk phase [6, 7], and this protein is used here as a representative case. In native states of cytochrome c, the heme group in the protein is covalently attached to the histidine (His) 18 residue and the methionine (Met) 80 residue. A number of kinetic studies suggest that under denaturing conditions the linkage of the heme group to Met 80 dissociates and is replaced by linkage to one of the other available histidine residues [8, 9]. This ligation of the heme by the second histidine is important in understanding the structural change or function of the protein under denaturing conditions. Godbole et al. [10, 11] studied the proton-mediated heme ligation equilibrium of yeast iso-1-cytochrome c (cytochrome c from *Saccharomyces cerevisiae*; Cyt c, Aldrich) under denaturing conditions. According to their studies, the H^+ ion protonates the nitrogen atom on histidine in Cyt c, causing the bond between the histidine nitrogen atom and the heme iron atom to break, which leads to a marked change in the conformation of the molecule. This conformational change of the protein at an interface has not been studied, and the reversible occurrence of the same phenomenon on a solid surface may facilitate its further application as a sensor or a switch. To test this possibility, we self-assembled Cyt c on spherical gold nanoparticles and investigated the pH-induced conformational change using a UV-VIS spectrophotometer. We chose gold nanoparticles because they are simple to prepare, easy to control, and cost effective. In addition, biomaterial-nanoparticle conjugations have been well studied using their optical and electronic properties [12–14].

SPR measurements of the refractive index (RI) at each pH were compared to the corresponding color of the Cyt c-coated nanoparticle solutions as represented by the wavelength of maximum absorbance. The color change of the nanoparticles with pH was found to closely mimic the SPR data. This fact suggests that protein-coated gold nanoparticles can be used to investigate the conformational change of proteins on a solid-liquid interface. The optical properties of colloidal nanoparticles have been used to explain the interactions between particles based on the specificity of complementary DNA strands [15–18] and to interpret conformational change in an oligonucleotide [19] and phase transition of a biopolymer [20]. To the best of our knowledge, however, gold nanoparticles have not been previously used to investigate the folding and unfolding of proteins.

Results

Color Change of Protein-Coated Au Nanoparticles

To investigate the proton-mediated heme ligation of Cyt c bound to Au nanoparticles, we prepared solutions of gold nanoparticles and then coated them with optimal levels of Cyt c as described in Experimental Procedures. After the gold nanoparticles were fully saturated with Cyt c, the pH of the solution was varied from 10.1 to 4.0 by drop-wise addition of hydrochloric acid (HCl, Fisher Scientific). This procedure was repeated separately on solutions of bare gold particles. Figure 1 provides visual evidence for the effect of pH on the nanoparticle solutions. The bare gold nanoparticle solutions in Figure 1A show no change from the original color, whereas the Cyt c-coated particles in Figure 1B display obvious color variation around pH 6. Absorption spectra were collected for each bare nanoparticle solution and each coated nanoparticle solution. The spectra for the bare gold particle solutions show peaks with a maximum absorbance at 525 nm regardless of the pH of the solution, whereas the spectra for the coated nanoparticles have absorption peaks that shift from 528 nm at high pH to 611 nm as the pH decreases to 4.0.

*Correspondence: zare@stanford.edu

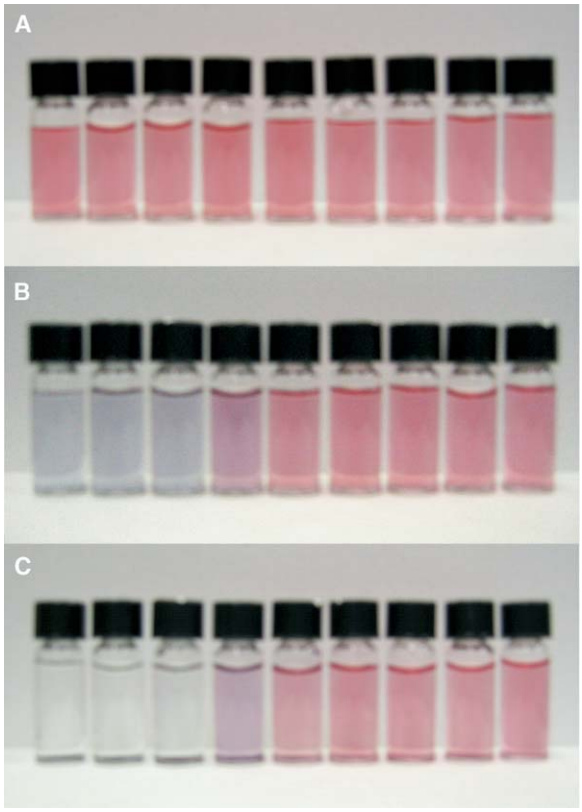

Figure 1. Visual Evidence of the Effect of pH on a Gold Nanoparticle Solution

(A) Color of Au nanoparticle solutions.
(B) Color of Cyt c-coated nanoparticle solutions at different pHs right after mixing (before precipitation). The pH values for vials, reading from left to right, are 4.0, 5.0, 5.5, 6.2, 6.7, 7.2, 8.3, 9.2, and 10.1.
(C) Color of Cyt c-coated nanoparticle solutions at different pHs after 24 hr (after precipitation).

The Cyt c-coated particles at low pH become more dilute over time and eventually precipitate after 24 hr. Those at a pH value of 6.2 or greater stay in solution for longer than one week (Figure 1C). Figure 2 presents transmission electron microscopy (TEM) images taken of Cyt c-coated particles from pH 4 and 10.1 solutions after each solution has been allowed to stand for more than 24 hr. The Cyt c-coated particles from the pH 4 solution appear in a clump (Figure 2A), having apparently aggregated to a much greater extent than Cyt c-coated particles from the pH 10.1 solution, which maintain a uniformly dispersed spherical shape (Figure 2B).

SPR Signal Change of Protein-Coated Au Films

For comparison, we designed a similar experimental system with a Cyt c layer bound to an Au film and used a commercial SPR sensor (Spreeta, Texas Instruments, Dallas, TX) to monitor changes of RIs in the protein layer as a function of the pH of the solution that flowed over the surface (described in Experimental Procedures). The RIs for bare Au increase from 1.33304 to 1.33316 with increasing pH while those for Cyt c-Au decrease from 1.33858 to 1.33810 as shown in Figure 3A. The RI change for bare Au (circles in Figure 3A) results from the RI differences among the pH-controlled solutions, which were set by either sodium hydroxide (NaOH, Mallinckrodt) or hydrochloric acid in deionized water. Assembly of the Cyt c layer under neutral pH conditions results in an RI jump from 1.333 to 1.338. In addition, the RI difference at low pH versus high pH for the assembled monolayer (squares in Figure 3A) is enhanced 3.5 times more than the RI difference for bare Au (circles in Figure 3A), and the RI decreases with increasing pH. These two trends strongly suggest conformational changes in the protein layer and lend credence to the assumption that the pH-mediated heme ligation equilibrium occurs in Cyt c on an Au surface in the same manner as in bulk solution.

The reversibility of the pH-driven RI change was tested for the Cyt c-Au SPR surface. Solutions at pH 4 and pH 10.7 were passed over the surface repeatedly. The procedure was also performed on a bare Au surface for comparison. Figure 3B shows the SPR signal obtained from six sequential injections of solutions at pH 4 and pH 10.7. The observed changes were quite reproducible, from which we conclude that Cyt c on Au folds and unfolds reversibly as a function of pH. The slight decrease in RI seen after injection of pH 4 solution is thought to be caused by the interference of air between solution injections. The signal tail after each injection of high pH solution indicates that the rate of unfolding is faster than that of folding, perhaps because of the competition between the N-terminal amino group and a histidine for heme ligation [11]. Nevertheless, the Cyt c molecules return perfectly to their folded state after each cycle.

Theoretical Consideration about Conformational Change of Cyt c on Au Surfaces

The optical properties of nanoparticles can be described using Mie scattering theory [21]. For a coated

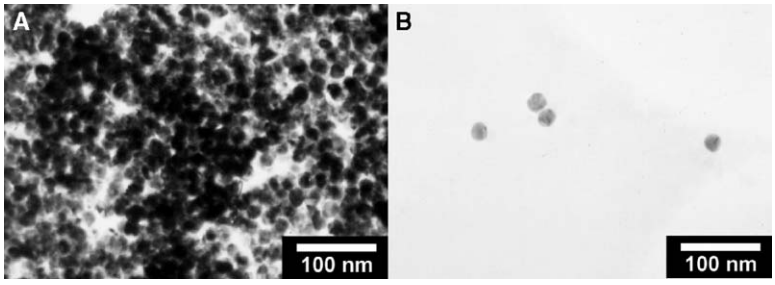

Figure 2. TEM Pictures of Cyt c-Coated Nanoparticles

(A) Cyt c-coated nanoparticles in pH 4.
(B) Cyt c-coated nanoparticles in pH 10.2. The Cyt c-coated nanoparticles remain monodispersed at high pH but aggregate and eventually precipitate at low pH.

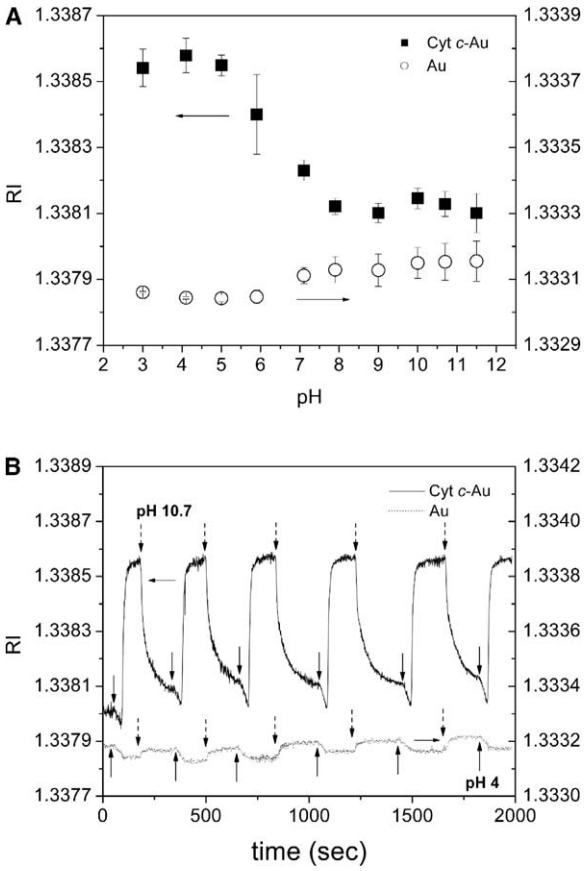

Figure 3. SPR Data for Both Bare Au and Cyt c-Au

(A) Refractive index (RI) measured on both bare Au (open circles) and Cyt c-Au (solid squares). The RI for bare Au increases as pH increases while that for Cyt c-Au decreases. The arrows point to the vertical axis associated with each data set.

(B) Reversibility and reproducibility of the SPR signal of Cyt c bound to Au. The conformational change of Cyt c on Au was reversible and reproducible when the pH of the solution in contact with the gold film was repeatedly varied from pH 4 to pH 10.7. Solid arrows and dotted arrows represent injection times of pH 4 and pH 10.7 solutions, respectively. The vertical axis on the left is for Cyt c bound to Au whereas the vertical axis on the right is for bare Au.

nanoparticle, the extinction efficiency is expressed by

$$Q_{ext} = \frac{8r\pi(\epsilon_m)^{1/2}}{\lambda} \mathrm{Im} \times \left(\frac{(\epsilon_2 - \epsilon_m)(\epsilon_1 + 2\epsilon_2) + f(\epsilon_1 - \epsilon_2)(\epsilon_m + 2\epsilon_2)}{(\epsilon_2 + 2\epsilon_m)(\epsilon_1 + 2\epsilon_2) + f(2\epsilon_2 - 2\epsilon_m)(\epsilon_1 - \epsilon_2)} \right), \quad (1)$$

where ϵ_1, ϵ_2, and ϵ_m are the complex dielectric functions of the particle core, the surface coating, and the medium, respectively, and *f*, *r*, and λ represent the fraction of the total particle volume occupied by the core, the particle radius, and the wavelength of the incident light, respectively. The calculation of Q_{ext} for the coated nanoparticles requires information about the dielectric constants of the Cyt c layer (ϵ_2) at each wavelength of incident light. Unfortunately, this information is difficult to determine and therefore is known for only a few materials. Moreover, the pH-induced conformational change of the protein complicates estimation of these parameters. Instead, we interpreted the phenomenon with angle-resolved SPR data obtained after coating the protein on an Au film.

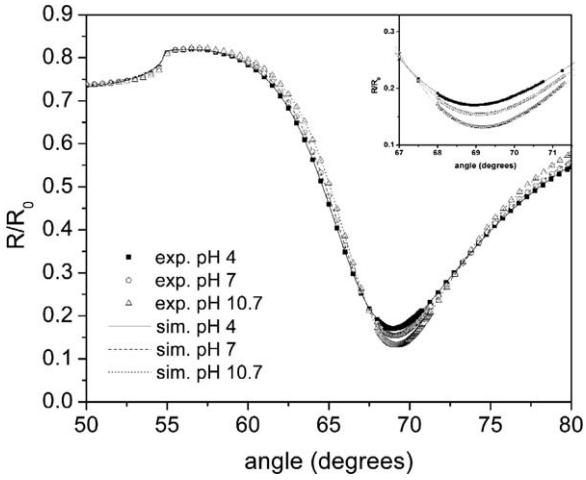

Figure 4. Experimental Angle-Resolved SPR Signals for Three Different pH Conditions

Solid squares, open circles, and open triangles are for pH 4, pH 7, and pH 10.7, respectively. The best fitting simulation data for obtaining dielectric constants and thickness of the Cyt c layer is represented by a solid line for pH 4, a dashed line for pH 7, and a dotted line for pH 10.7. The inset shows a magnified portion of this figure over the range from 67°C to 71.5°C.

We prepared the Au surface and measured angle-resolved SPR signals for different pH values as described in Experimental Procedures. The squares, circles, and triangles in Figure 4 represent experimental angle-resolved SPR data from the Cyt c-Au surface at pH 4, pH 7, and pH 10.7, respectively. The inset in Figure 4 magnifies the SPR data near the SPR angles (minimum R/R_0) as a function of pH. On the basis of the experimental data, the dielectric constant and thickness of the Cyt c monolayer were calculated for the three different pHs using a theory described elsewhere [22, 23]. For the multilayer model employed here, n represents the layer number, which is given the value of 0, 1, 2, 3, or 4 for the SF10 prism, Cr binder layer, Au layer, Cyt c layer, and solution at a fixed pH. For each layer, the layer thickness is denoted by d_n and the real and imaginary parts of the dielectric constant are denoted by ϵ'_n and ϵ''_n, respectively. The optical properties of layers 0, 1, and 2 were obtained from the literature [24], and that of the fourth layer was calculated from the RI data of each pH solution (circles in Figure 3A). Using these parameters as an initial starting condition, d_1, d_2, d_3, ϵ_2', ϵ_2'', ϵ_3', and ϵ_3'' were calculated by optimizing the simulated line fits to the experimental data with an iteration method in Winspall (Fresnel equation solver, MPIP, Germany). Figure 4 shows curves fitted to the experimental data under each condition, and the estimated parameters are listed in Table 1. The calculated thicknesses, d_1 and d_2, agree well with the quartz crystal microbalance (QCM) data (1 nm for Cr, 50 nm for Au). The thickness of the Cyt c layer, d_3, is larger at low

Table 1. Dielectric Constant and Thickness of Each Layer Calculated for Three Different pH Values

pH	ϵ_0	ϵ_1'	ϵ_1''	ϵ_2'	ϵ_2''	ϵ_3'	ϵ_3''	ϵ_4	d_1(nm)	d_2(nm)	d_3(nm)
4.0						1.4309	0.8352	1.7770	1.00	50.71	3.18
7.0	2.9687	–6.8992	30.3456	–10.2773 ± 0.1697	1.2766 ± 0.1864	1.3334	1.0797	1.7772	1.00	50.77	2.58
10.7						1.4006	1.5041	1.7774	1.00	50.76	2.36

pH than at high pH. The increase is about 1 nm, which supports the proton-mediated heme ligation equilibrium of Cyt c attached to the Au surface. In addition to the change in thickness, the imaginary part of the dielectric constant, ϵ_3'', decreases. This behavior suggests indirectly that the increase of d_3 dilutes the concentration of the layer. This observation again supports the contention that Cyt c on the Au surface unfolds as the pH decreases. This same phenomenon is expected to occur in Cyt c assembled on Au nanoparticles.

Discussion

A surface plasmon (SP) is a collective excitation of the electrons at the interface between a conductor and an insulator. Absorption of light by the SPs of small metallic particles accounts for the colorful appearance of suspensions of these particles, and the color is affected by the size and the extent of aggregation of the particles [25–27]. Both the attachment of Cyt c on Au nanoparticles and the conformational change of the protein attached on Au are expected to affect SPs, which should result in color changes in the solutions. The maximum absorbance wavelength (λ_{max}) for the Au nanoparticle solution at pH 11.0 is 525 nm, and the λ_{max} for the Cyt c-coated nanoparticle solution at pH 11.0 is 528 nm, a 3 nm increase. This difference arises from the presence of the ~2.5 nm-thick Cyt c layer, which creates an effective increase in the size of the nanoparticles. Changes in the layer thickness arising from pH-driven conformational change are on the order of 0.8 nm (see Table 1), and thus conformational changes in protein-coated nanoparticles are expected to appear as changes smaller than 3 nm in the absorption wavelength. However, Cyt c-coated Au nanoparticle solutions exhibit obvious color changes of nearly 80 nm, as shown in Figure 1B, and this big difference is accounted for by particle aggregation.

Particle aggregation is seen as a red shift in the color of a Au nanoparticle solution arising from the formation of absorption bands in the extinction spectrum at long wavelengths. These absorption bands are caused by electric dipole-dipole interaction and coupling between plasmons of neighboring particles inside the aggregates, provided that the interparticle distance inside the aggregate is smaller than the particle diameter. Figures 1C and 2 show the particle aggregation for this study. Interestingly, only Cyt c-coated particles in fully unfolded regions (low pH) precipitate. The Cyt c samples in intermediate regions and native-like regions (high pH), as well as uncoated Au nanoparticles in all regions, retain their original color even after a week. The unfolding of Cyt c is likely to cause the formation of a network between Cyt c-coated particles located close together. Reversibility studies performed on Cyt c-coated particles support this conclusion. Immobilized Cyt c on an Au film demonstrated reversible conformational change as shown in Figure 3B. However, the Cyt c-coated nanoparticles did not exhibit the same degree of reversibility. When the pH of a sample solution was repeatedly changed between 10.7 and 4.0 on a short time scale (approximately once per minute), the Cyt c-coated particle solution changed from red at high pH to blue at low pH for three repetitions. However, for subsequent pH changes, the solution color at high pH only partially returned to its original red color, retaining a slight blue character. Absorption data for these samples show a λ_{max} of 528 nm at high pH for the first iteration that shifts gradually to 577 nm for the fifth. Reversibility experiments performed at long time scales (1 day or longer) show no color change after the initial adjustment to pH 4.0. This result indicates that the precipitated particles form networks that do not dissociate, even under high pH conditions. The exact causes of the aggregation have not been established, but they likely involve hydrophobic interaction, in the same way as was observed for elastin bound to gold nanoparticles [20]. Nevertheless, we can interpret this behavior as demonstrating that the unfolding and refolding of Cyt c attached to the Au particle is reversible but is moderated by the irreversible formation of a bonded network between the unfolded Cyt c-coated Au particles.

Normalized λ_{max} values taken from absorption data for the Cyt c-coated nanoparticle solutions are presented in Figure 5, along with RI data for the Cyt c-Au film. The SPR signal closely follows the color change of the protein-coated Au nanoparticles except near pH 7. This deviation results from the overlap of the absorption peak of small aggregate clusters and the peak from lone particles remaining in solution in the intermediate pH region. At high pH, proteins on both the Au film and Au nanoparticles are in a folded state and they do not aggregate. In this pH region, the two data sets follow the same line. Near pH 7, particle aggregation by unfolded proteins on nanoparticles starts to occur but lone particles dominate in the solution. Since the absorption peak for lone particles overlaps the absorption peak from the aggregated particles in this region, the recorded λ_{max} value remains close to the lone particle absorption peak value. As the pH decreases and more aggregate clusters form, the aggregate absorbance peak increases in intensity and shifts into high wavelengths while the absorption peak diminishes for lone particles. Near pH 6, the aggregate absorption peak has shifted far enough into the high wavelength region that it is distinguishable as a separate peak but is never fully resolved. Here, absorption data again closely approach the RI data. At low pH, where the proteins are all in their unfolded state, the RI and absorption data again flatten out.

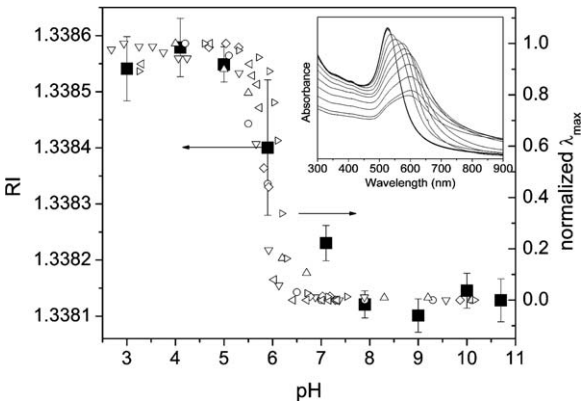

Figure 5. Comparison of the SPR Signal from Cyt c Bound to a Flat Gold Surface with the Wavelength of Maximum Absorption, λ_{max}, in the Visible Spectrum of Cyt c-Coated Nanoparticle Cluster

Each symbol represents one set of experiments. The arrows point to the vertical axis associated with each data set. The inset shows a representative absorption spectra for the case of the data set denoted by the symbol △. The pH values read 10.16, 7.53, 7.14, 6.71, 6.29, 6.19, 6.10, 6.03, 5.93, 5.71, 5.30, 4.60, and 3.25 from top to bottom. The first four spectra in the inset coincide.

We have explored proton-mediated conformational change of a protein on gold surfaces using the SPR technique as well as on gold nanoparticles using absorption spectroscopy. This behavior might be different depending on initial conditions such as compactness of proteins on the surface. A recent publication by Jiang et al. [28] supports this contention. They studied the effect of binding bovine heart cytochrome c on two different sizes of colloidal gold nanoparticles. These proteins bind electrostatically (not covalently) as dimers, and the changes in color (absorption spectrum), circular dichroism, and FTIR are interpreted in terms of structural changes of the dimer with packing density. Further work is necessary to learn about the effect of crowding on the protein structure.

Significance

We have described the possibility of using gold nanoparticles as a colorimetric sensor for protein conformational change. Although the color change results not from conformational change itself but from particle aggregation induced by unfolding of the protein, the color change of Cyt c-coated particle solution mimics the RI change of a Cyt c-Au film quite well. This fact suggests that the aggregation of gold nanoparticles is directly related to the conformation of the attached protein and that gold nanoparticles can easily and reliably be used to create a simple and inexpensive sensor for protein conformation change.

Experimental Procedures

Preparation of 19 nm Gold Nanoparticles

We followed a procedure for preparing gold nanoparticles described previously [29, 30]. The particles were prepared by boiling 200 ml of aqueous 0.005% (w/w) hydrogen tetrachloroaurate(III) trihydrate ($HAuCl_4 \cdot 3H_2O$, Aldrich) stirred vigorously in a flask connected to a water-cooling column and subsequently adding 15.3 mg of sodium citrate ($Na_3C_6H_5O_7 \cdot 2H_2O$, Mallinckrodt). Once the color of the solution began to change, the heat was turned off and the solution was allowed to cool overnight to room temperature. The solution was filtered by syringe filter (200 nm pore size, Whatman). The diameter of the nanoparticles was found to be 19 nm by transmission electron microscopy (CM20 FEG-TEM, Philips). In the procedure, any H_2O used was purified to more than 18 MΩ using a Milli-Q water system (Millipore).

Preparation of Cyt c-Coated Gold Nanoparticles

We initially prepared different samples of varying ratios between the Cyt c solution (3.5 μM in potassium phosphate buffer of pH 7.2) and the nanoparticle solution, ranging from 100:1 to 1:100 by volume. Before mixing, the pH of the nanoparticle solution was adjusted to 11.0 to prevent Cyt c from being acid denatured during self assembly, since the thiol-gold bond results in the release of protons, Cyt c-SH + Au → Cyt c-SAu + H^+. After Cyt c was vigorously mixed with the nanoparticle solution, the samples were left overnight for full saturation. The pH was then adjusted to 11.0 again, and absorption spectra for each sample ratio were measured. The absorbance peaks observed at 411 nm belong to Cyt c, and the peaks observed at 528 nm belong to gold nanoparticles. The ratio where the peaks at 411 nm disappeared when they were scanned from 100:1 to 1:100 samples was selected as the optimum ratio between Cyt c and the nanoparticle solution. The optimum ratio determined for the nanoparticles in this study is 1:30, and nanoparticles coated at this ratio were used in all experiments.

RI Measurement

Prior to RI measurement, the SPR instrument (Spreeta) was calibrated at room temperature to be 1.000 RIU in air and 1.333 RIU in water. The RIs for each pH solution (3.0, 4.1, 5.0, 5.9, 7.1, 7.9, 9.0, 10.0, and 10.7) were measured while passing the solutions over the gold surface at the fixed rate of 84 μl/min using the peristaltic pump (Watson Marlow Alitea, Stockholm, Sweden). The surface was then washed with water for cleaning, and it was modified with 35 μM Cyt c dissolved in 10 mM potassium phosphate buffer (pH 7.2). The existence of a thiol-linker from the single cystein at position 102 in the protein enables its easy and strong binding to an Au surface. The change in the SPR signal was initiated by the contact of Cyt c on gold, and continued until the surface was fully saturated with Cyt c. After saturation, the surface was washed with buffer and water several times to remove nonspecifically bound Cyt c. Thereafter, the RIs for the same set of pH solutions were measured on the Cyt c-modified gold surface (Cyt c-Au). For each experiment, we used a 3.5 μl volume flow cell that was built in house.

Measurement of Angle-Resolved SPR Signals

A 50 nm gold film followed by a 1 nm Cr adhesive layer was deposited on an SF10 glass (Schott Glass Technology) under high vacuum (~5–6 × 10^{-7} mbar) by an evaporator (Auto 306, Edwards High Vacuum International). The thickness was monitored using a quartz crystal microbalance (QCM). The Au surface was immersed in 35 μM Cyt c solution dissolved in 10 mM potassium phosphate buffer (pH 7.2) for 24 hr to make sure that it was fully saturated. Then, it was washed with buffer and water to remove noncovalently bonded molecules and dried with nitrogen. Finally, it was mounted on the rotational stage of a home-made SPR system [31] with a prism and a cell containing water. The reflectivity was then measured as a function of angle under three pH conditions (pH 4, pH 7, and pH 10.7).

Acknowledgments

This work is supported by the National Science Foundation under grant number MPS-0313996.

Received: November 14, 2004
Revised: January 28, 2005
Accepted: January 31, 2005
Published: March 25, 2005

References

1. Harper, S.M., Neil, L.C., and Gardner, K.H. (2003). Structural basis of a phototropin light switch. Science *301*, 1541–1544.
2. Ohba, S., Hosomi, H., and Ito, Y. (2001). In situ X-ray observation of pedal-like conformational change and dimerization of trans-cinnamamide in cocrystals with phthalic acid. J. Am. Chem. Soc. *123*, 6349–6352.
3. Zhu, X., Yan, D., and Fang, Y. (2001). In situ FTIR spectroscopic study of the conformational change of isotactic polypropylene during the crystallization process. J. Phys. Chem. B *105*, 12461–12463.
4. Gupta, R., and Ahmad, F. (1999). Protein stability: functional dependence of denaturational gibbs energy on urea concentration. Biochemistry *38*, 2471–2479.
5. Sadana, A. (1992). Protein adsorption and inactivation on surfaces. Influence of heterogeneities. Chem. Rev. *92*, 1799–1818.
6. Muthukrishnan, K., and Nall, B.T. (1991). Effective concentrations of amino acid side chains in an unfolded protein. Biochemistry *30*, 4706–4710.
7. Fink, A.L., Calciano, L.J., Goto, Y., Kurotsu, T., and Palleros, D.R. (1994). Classification of acid denaturation of proteins: intermediates and unfolded states. Biochemistry *33*, 12504–12511.
8. Elöve, G.A., Bhuyan, A.K., and Roder, H. (1994). Kinetic mechanism of cytochrome *c* folding: involvement of the heme and its ligands. Biochemistry *33*, 6925–6935.
9. Sosnick, T.R., Mayne, L., Hiller, R., and Englander, S.W. (1994). The barriers in protein folding. Nat. Struct. Biol. *1*, 149–156.
10. Godbole, S., and Bowler, B.E. (1999). Effect of pH on formation of a nativelike intermediate on the unfolding pathway of a Lys 73 → His variant of yeast iso-1-cytochrome c. Biochemistry *38*, 487–495.
11. Godbole, S., Hammack, B., and Bowler, B.E. (2000). Measuring denatured state energetics: deviations from random coil behavior and implications for the folding of iso-1-cytochrome c. J. Mol. Biol. *296*, 217–228.
12. Katz, E., Shipway, A.N., and Willner, I. (2004). Biomaterial-nanoparticle hybrid systems: synthesis, properties, and applications. In Nanoparticles from Theory to Application, G. Schmid, ed. (Germany: Wiley-VCH), pp. 368–421.
13. Daniel, M.-C., and Astruc, D. (2004). Gold nanoparticles: assembly, supramolecular chemistry, quantum-size-related properties, and applications toward biology, catalysis, and nanotechnology. Chem. Rev. *104*, 293–346.
14. Verma, A., Simard, J.M., and Rotello, V.M. (2004). Effect of ionic strength on the binding of α-chymotrypsin to nanoparticle receptors. Langmuir *20*, 4178–4181.
15. Mirkin, C.A., Letsinger, R.L., Mucic, R.C., and Storhoff, J.J. (1996). A DNA-based method for rationally assembling nanoparticles into macroscopic materials. Nature *382*, 607–609.
16. Goodrich, G.P., Helfrich, M.R., Overberg, J.J., and Keating, C.D. (2004). Effect of macromolecular crowding on DNA:Au nanoparticle bioconjugate assembly. Langmuir *20*, 10246–10251.
17. Maxwell, D.J., Taylor, J.R., and Nie, S. (2002). Self-assembled nanoparticle probes for recognition and detection of biomolecules. J. Am. Chem. Soc. *124*, 9606–9612.
18. Lu, Y., and Liu, J. (2004). Accelerated color change of gold nanoparticles assembled by DNAzymes for simple and fast colorimetric Pb^{2+} detection. J. Am. Chem. Soc. *126*, 12298–12305.
19. Park, S., Brown, K.A., and Hamad-Schifferli, K. (2004). Changes in oligonucleotide conformation on nanoparticle surfaces by modification with mercaptohexanol. Nano Lett. *4*, 1925–1929.
20. Nath, N., and Chilkoti, A. (2001). Interfacial phase transition of an environmentally responsive elastin biopolymer adsorbed on functionalized gold nanoparticles studied by colloidal surface plasmon resonance. J. Am. Chem. Soc. *123*, 8197–8202.
21. Bohren, C.F., and Huffman, D.R. (1998). Absorption and Scattering of Light by Small Particles (New York: John Wiley & Sons).
22. Chah, S., Hutter, E., Doy, R., Fendler, J.H., and Yi, J. (2001). The effect of substrate metal on 2-aminoethanethiol and nanoparticle enhanced surface plasmon resonance imaging. Chem. Phys. *272*, 127–136.
23. Hutter, E., Fendler, J.H., and Roy, D. (2001). Surface plasmon resonance method for probing interactions in nanostructures: CdS nanoparticles linked to Au and Ag substrates by self-assembled hexanedithiol and amionoethanethiol monolayers. J. Appl. Phys. *90*, 1977–1985.
24. Weaver, J.H., and Frederikse, H.P.R. (2002). Optical properties of selected elements.. In CRC Handbook of Chemistry and Physics, D.R. Lide, ed. (Boca Raton, FL: CRC Press Inc.), pp. 12.133–12.156.
25. Link, S., and El-Sayed, M. (1999). Spectral properties and relaxation dynamics of surface plasmon electronic oscillations in gold and silver nanodots and nanorods. J. Phys. Chem. B *103*, 8410–8426.
26. Kelly, K.L., Coronado, E., Zhao, L.L., and Schatz, G.C. (2003). The optical properties of metal nanoparticles: the influence of size, shape, and dielectric environment. J. Phys. Chem. B *107*, 668–677.
27. Jensen, T.R., Schatz, G.C., and Van Duyne, R.P. (1999). Nanosphere lithography: surface plasmon resonance spectrum of a periodic array of silver nanoparticles by ultraviolet-visible extinction spectroscopy and electrodynamic modeling. J. Phys. Chem. B *103*, 2394–2401.
28. Jiang, X., Jiang, J., Jin, Y., Wang, E., and Dong, S. (2005). Effect of colloidal gold size on the conformational changes of adsorbed cytochrome *c*: probing by circular dichroism, UV-visible, and infrared spectroscopy. Biomacromolecules *6*, 46–53.
29. Handley, D.A. (1989). Methods for synthesis of colloidal gold. In Colloidal Gold: Principles, Methods and Applications, M.A. Hayat, ed. (San Diego: Academic Press), pp. 13–32.
30. Chah, S., Fendler, J.H., and Yi, J. (2002). Nanostructured gold hollow microspheres prepared on dissolvable ceramic hollow sphere templates. J. Colloid Interf. Sci. *250*, 142–148.
31. Chah, S., Kumar, C.V., Hammond, M.R., and Zare, R.N. (2004). Denaturation and renaturation of self-assembled yeast iso-1-cytochrome *c* on Au. Anal. Chem. *76*, 2112–2117.